Supporting information

A highly connected (5,5,18)-c trinodal MOF with a 3D diamondoid inorganic connectivity: Tunable luminescence and white-light emission

Zhongyuan Zhou,[a,b] Qipeng Li,[a] Yunhu Han,[a] Xiushuang Xing,[a,b] and Shaowu Du[a]*

[a] State Key Laboratory of Structural Chemistry, Fujian Institute of Research on the Structure of Matter, Chinese Academy of Sciences, Fuzhou, Fujian 350002, P. R. China. E-mail: swdu@fjirsm.ac.cn

[b] College of Chemistry, Fuzhou University, Fuzhou, Fujian, 350108, P. R. China

Table S1 Selected bonds lengths (Å) of **1**

Cd1—O2^{i}	2.264 (3)	O3—K1^{viii}	2.851 (5)
Cd1—O2^{ii}	2.264 (3)	O3—K1^{v}	2.949 (5)
Cd1—O4^{iii}	2.289 (3)	O1—K1^{ix}	2.707 (4)
Cd1—O4	2.289 (3)	O1—K1^{x}	2.720 (4)
Cd1—N1^{iii}	2.330 (4)	O2—Cd1^{viii}	2.264 (3)
Cd1—N1	2.330 (4)	O2—K1^{viii}	2.855 (4)
K1—O1^{i}	2.707 (4)	K1—O4	2.898 (4)
K1—O1^{iv}	2.720 (4)	K1—O3^{ii}	2.851 (5)
K1—O2^{ii}	2.855 (4)	K1—O3^{v}	2.949 (5)

Table S2 Selected bond angles (°) of **1**

$O2^{i}$—Cd1—$O2^{ii}$	104.09 (19)	$O1^{i}$—K1—$O1^{iv}$	90.36 (11)
$O2^{i}$—Cd1—$O4^{iii}$	80.09 (12)	$O1^{i}$—K1—$O3^{ii}$	139.28 (15)
$O2^{ii}$—Cd1—$O4^{iii}$	101.36 (13)	$O1^{iv}$—K1—$O3^{ii}$	126.52 (13)
$O2^{i}$—Cd1—O4	101.36 (13)	$O1^{i}$—K1—$O2^{ii}$	98.45 (11)
$O2^{ii}$—Cd1—O4	80.09 (12)	$O1^{iv}$—K1—$O2^{ii}$	148.21 (16)
$O4^{iii}$—Cd1—O4	177.69 (18)	$O3^{ii}$—K1—$O2^{ii}$	60.50 (10)
$O2^{i}$—Cd1—$N1^{iii}$	151.11 (12)	$O1^{i}$—K1—O4	69.95 (13)
$O2^{ii}$—Cd1—$N1^{iii}$	86.63 (13)	$O1^{iv}$—K1—O4	94.12 (15)
$O4^{iii}$—Cd1—$N1^{iii}$	71.45 (12)	$O3^{ii}$—K1—O4	117.28 (11)
O4—Cd1—$N1^{iii}$	106.94 (13)	$O2^{ii}$—K1—O4	61.23 (10)
$O2^{i}$—Cd1—N1	86.63 (13)	$O1^{i}$—K1—$O3^{v}$	75.03 (14)
$O2^{ii}$—Cd1—N1	151.11 (12)	$O1^{iv}$—K1—$O3^{v}$	72.36 (13)
$O4^{iii}$—Cd1—N1	106.94 (13)	$O3^{ii}$—K1—$O3^{v}$	98.25 (12)
O4—Cd1—N1	71.45 (12)	$O2^{ii}$—K1—$O3^{v}$	139.42 (13)
$N1^{iii}$—Cd1—N1	96.79 (19)	O4—K1—$O3^{v}$	142.32 (12)

Symmetry codes: (i) $-y + 1/4, x - 1/4, z - 1/4$; (ii) $y + 3/4, -x + 3/4, z - 1/4$; (iii) $-x + 1, -y + 1/2, z$; (iv) $y + 3/4, -x + 1/4, -z - 3/4$; (v) $-x + 1, -y, -z - 1$; (vi) $y + 1/4, -x + 3/4, -z - 5/4$; (vii) $-y + 3/4, x - 1/4, -z - 5/4$; (viii) $-y + 3/4, x - 3/4, z + 1/4$; (ix) $y + 1/4, -x + 1/4, z + 1/4$; (x) $-y + 1/4, x - 3/4, -z - 3/4$.

Table S3 ICP analysis for **1** ⊃ **Eu** in different concentration of Eu^{3+}

Comp.	m_{Eu}^{3+}/mg	Solvent/ml	soak time/h	ICP/%
1 ⊃ **Eu1**	20	5	24	0.53
1 ⊃ **Eu2**	50	5	24	0.58
1 ⊃ **Eu3**	100	5	24	1.10
1 ⊃ **Eu4**	150	5	24	1.32
1 ⊃ **Eu5**	200	5	24	1.94

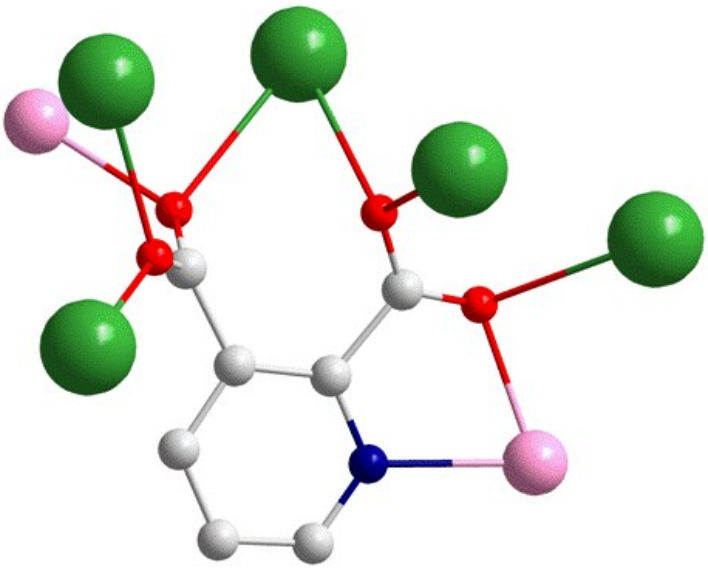

Fig.S1 The coordination of the ligand in compound **1**.

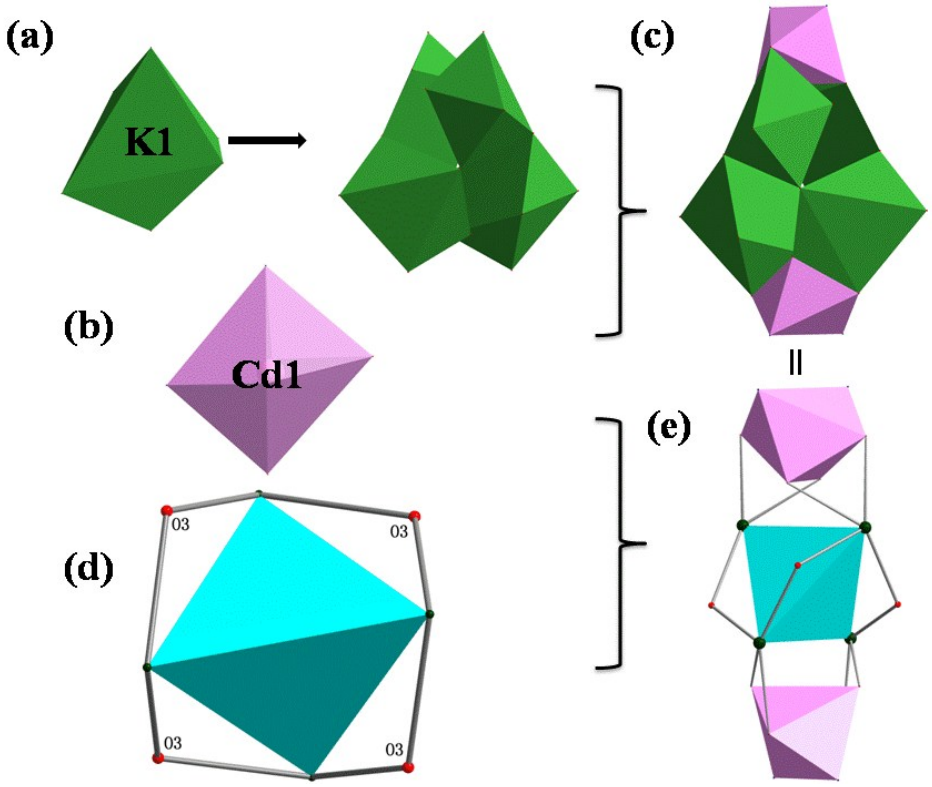

Fig. S2 View of the polyhedra of (a) K1 and $\{K_4\}$ cluster. (b) Cd1. (c) $\{Cd_2K_4\}$ cluster. (d) The $\{K_4\}$ cluster linked by four μ_2-O3 bridges. (e) The $\{Cd_2K_4\}$ cluster linked by μ_2-O2 and μ_2–O4.

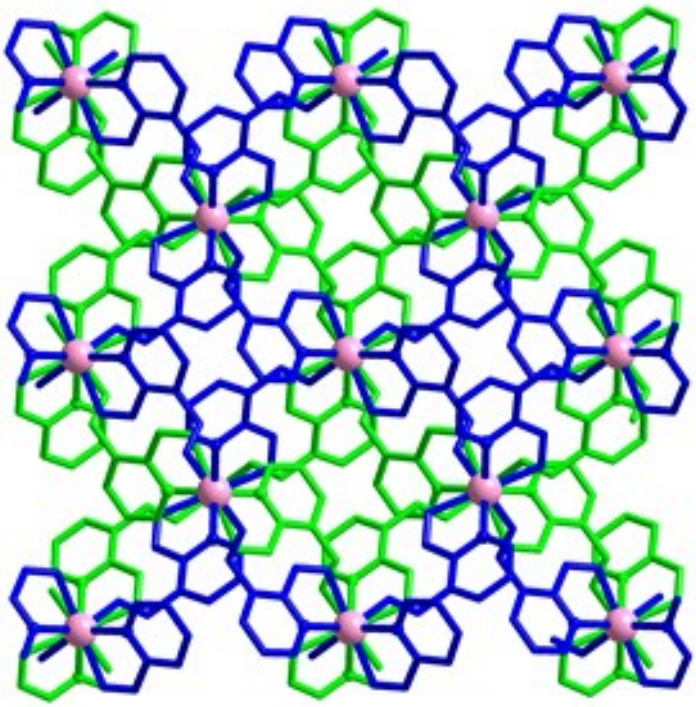

Fig. S3 The interpenetration of two independent 3D anionic frameworks in the absence of potassium ions.

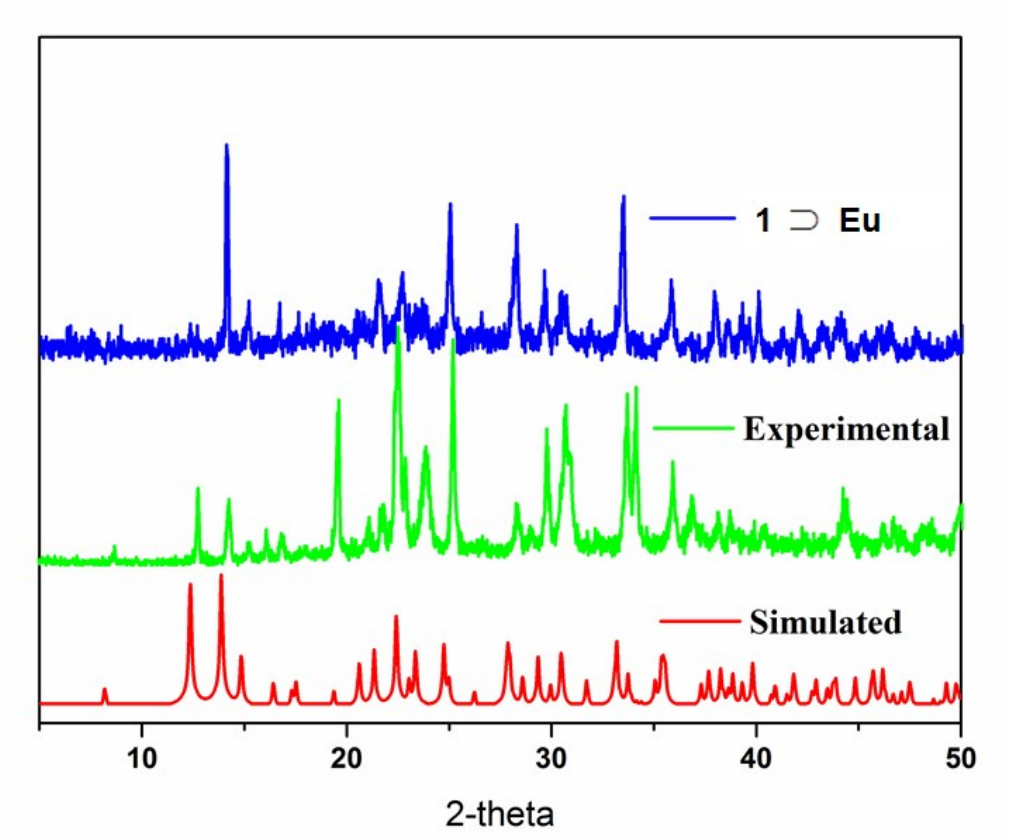

Fig. S4 Simulated and experimental XRD powder patterns for **1** and **1** ⊃ **Eu**.

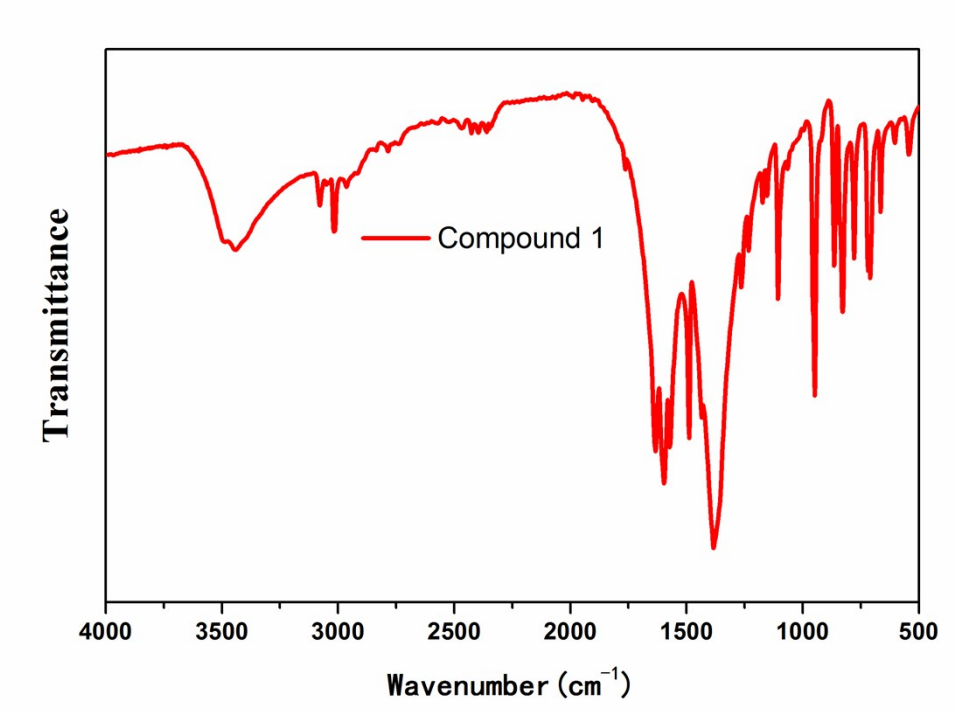

Fig. S5 View of the IR spectra of **1.**

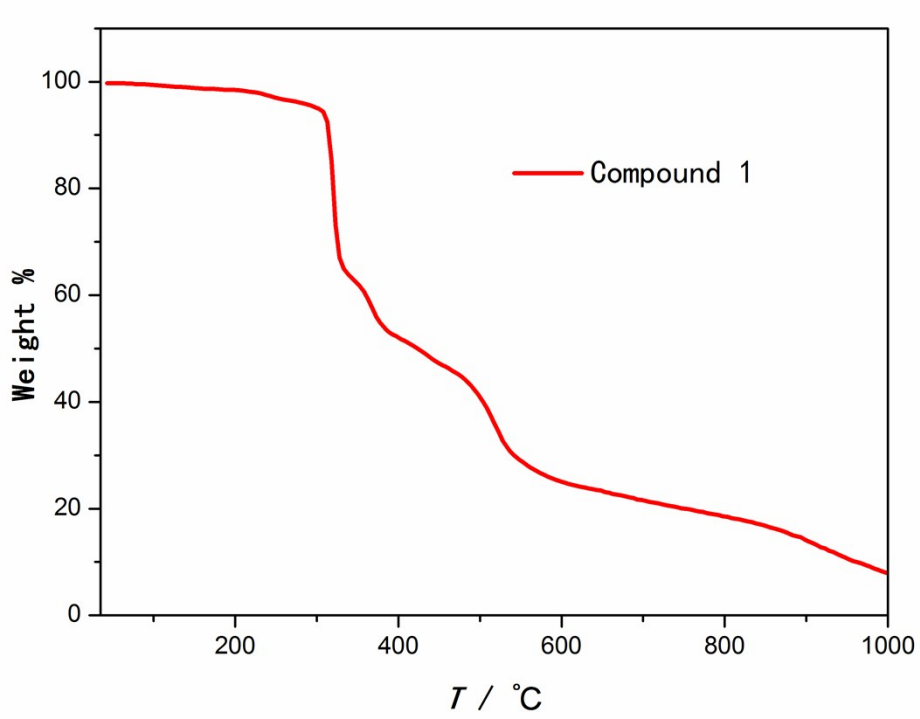

Fig. S6 TGA curve for compound **1**.

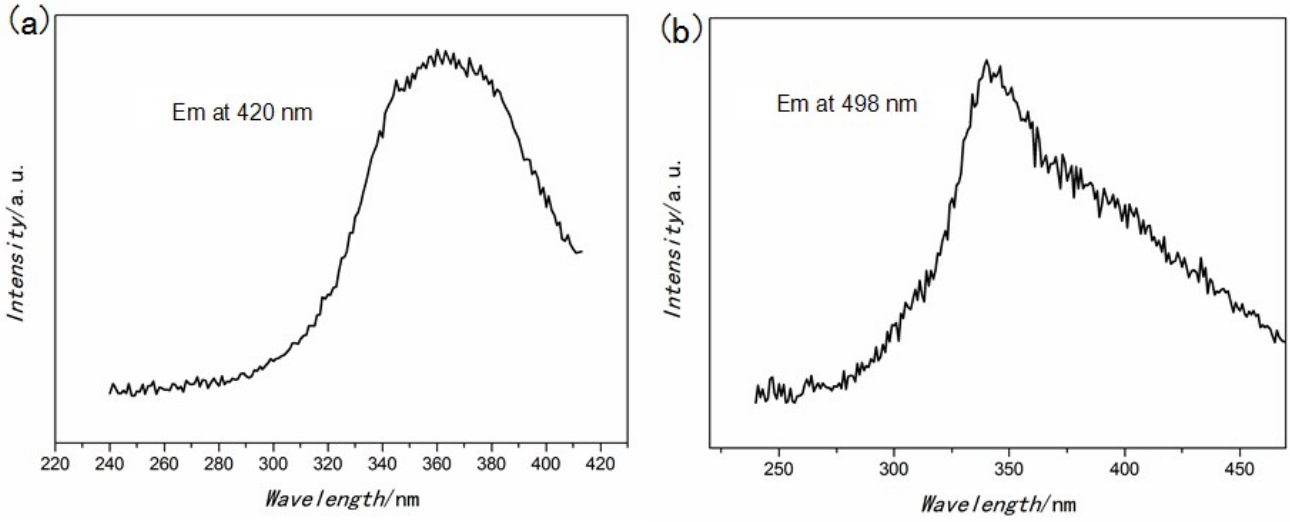

Fig. S7 Excitation spectra for the emission at 420 and 498 nm in the solid state of compound **1**.

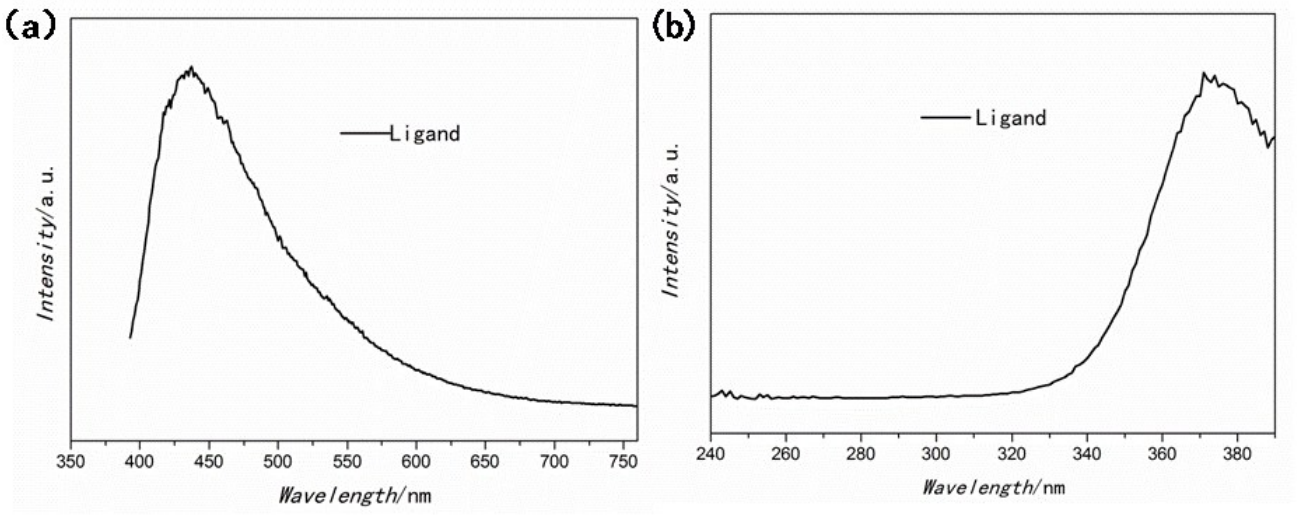

Fig. S8 The luminescence emission (a) and excitation (b) of the ligand 2,3-H_2PDC at room temperature.

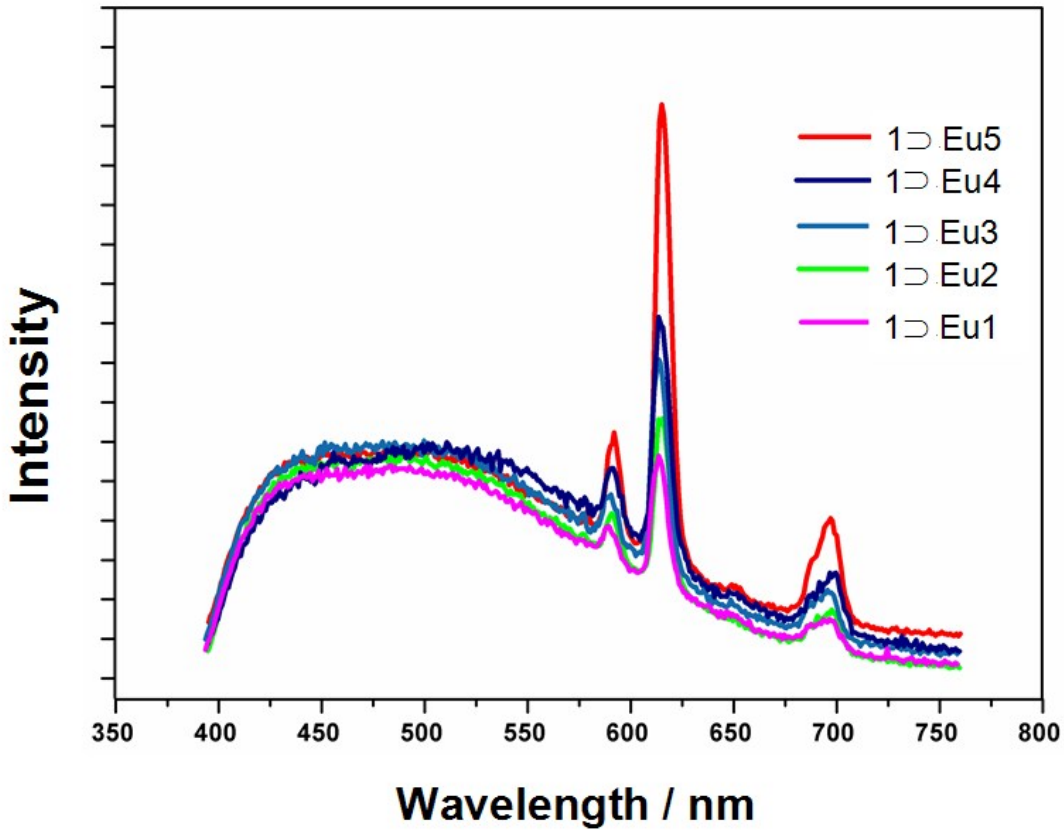

Fig. S9 The luminescence emission of **1 ⊃ Eu1** to **1 ⊃ Eu5** with different concentration of Eu^{3+}

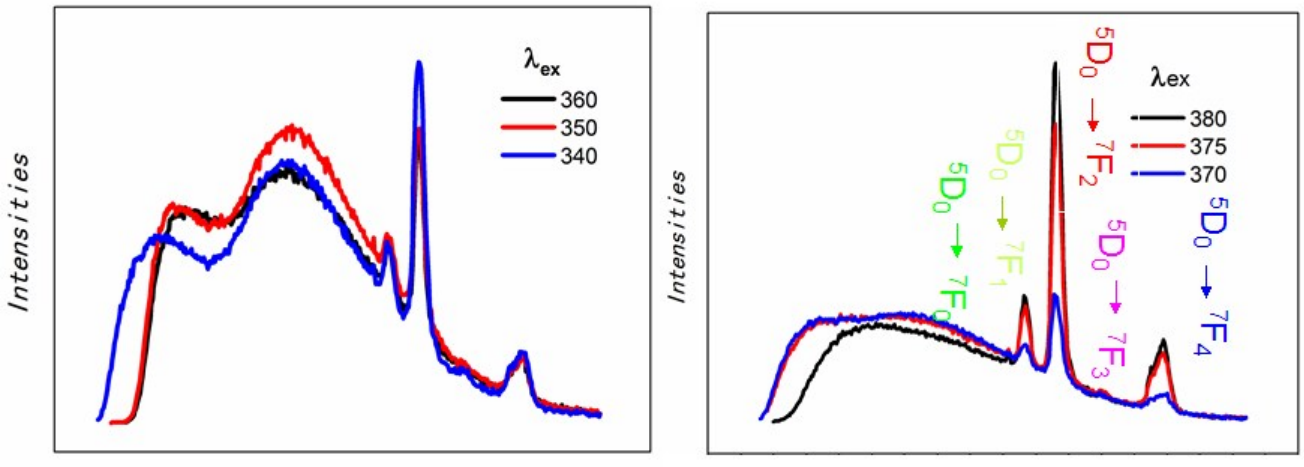

Fig. S10 Solid-state emission spectra of **1** ⊃ **Eu5** at λ_{ex} = 380, 375, 370, 360, 350 and 340 nm.